NANO LETTERS

2007
Vol. 7, No. 10
3128−3133

Layer-in-Layer Hierarchical Nanostructures Fabricated by Combining Holographic Polymerization and Block Copolymer Self-Assembly

Michael J. Birnkrant and Christopher Y. Li*

A. J. Drexel Nanotechnology Institute and Department of Materials Science and Engineering, Drexel University, Philadelphia, Pennsylvania 19104

Lalgudi V. Natarajan, Vincent P. Tondiglia, and Richard L. Sutherland

Science Applications International Corporation, 4031 Colonel Glenn Highway, Dayton, Ohio 45431

Pamela F. Lloyd

UES, Inc., 4401 Dayton-Xenia Road, Dayton, Ohio 45432

Timothy J. Bunning*

Air Force Research Laboratory, Materials & Manufacturing Directorate, Wright-Patterson Air Force Base, Ohio 45433

Received July 10, 2007; Revised Manuscript Received August 27, 2007

ABSTRACT

We report the combination of top-down and bottom-up nanomanufacturing techniques to fabricate active, hierarchically structured volume reflection gratings. Holographic polymerization (H-P) formed lamellar structures of ~200 nm in thickness, confining a block copolymer (BCP) to ~100 nm domains. Subsequently, the BCP self-assembles into nanolayers with a period of ~21 nm. We envisage that this approach opens a gateway to fabricating hierarchical nanostructures at different length scales.

Top-down and bottom-up represent two methods for manufacturing nanoscale materials. The top-down technique is approaching its theoretical limits, and processes such as e-beam lithography are costly as the feature size becomes smaller.[1,2] The feature size of the top-down method is usually limited by the optical sources as well as fabrication techniques; the limit for the current technology is a few tens of nanometers.[2] In contrast, the bottom-up method can easily reach nanometer-scale feature sizes when starting from tailored molecules.[1] One drawback of the bottom-up technique is its inability to achieve large-scale, defect-free structures, which are essential for nanoelectronic applications.[1] Furthermore, hierarchical structures with complex features at different length scales are of great interest because they ensure property control, transfer, and multifunctionality. Hierarchical structures are often difficult to fabricate because most of the nanomanufacturing techniques can only be used to produce structures at a certain narrow length scale.[3,4] Self-assembly could lead to hierarchical nanostructures by incorporating different ordering mechanisms in one system as reported.[5−8] However, the length scale is usually limited from subnanometer to a few tens of nanometers. The intrinsic defect problem of self-assembly also hinders its practical applications. One way to circumvent this technological hurdle is to combine the top-down and bottom-up methods in one system: the top-down technique fabricates long-range, large-scale ~100 nm features while self-assembly creates tailored finer scale 1−100 nm structures.

A few methods have been proposed to combine both manufacturing techniques. The so-called top-down assisted bottom-up approach was used to aid block copolymers (BCP)[9,10] and colloidal particle self-assembly[11] by patterning surfaces to achieve long-range ordering. In addition, the self-

* Corresponding author. E-mail: Chrisli@drexel.edu (C.Y.L.); Timothy.Bunning@wpafb.af.mil (T.J.B.). Telephone: 215-895-2083 (C.Y.L.); 937-255-9608 (T.J.B.). Fax: 215-895-6760.

10.1021/nl071673j CCC: $37.00
Published on Web 09/14/2007

Scheme 1. Schematic Representation of Hierarchical Nano Manufacturing by Combining H-P and BCP Self-assembly; (a) Syrup Containing Photopolymerizable Monomers, BCP, and Photoinitiators; (b) H-P Forms Ordered Structure on a ~200 nm Scale; (c) BCP Self-Assemblies in Nanodomains Created by H-P Structures; (d) A Variety of Different BCP Structures Could Be Confined in the H-P Layers

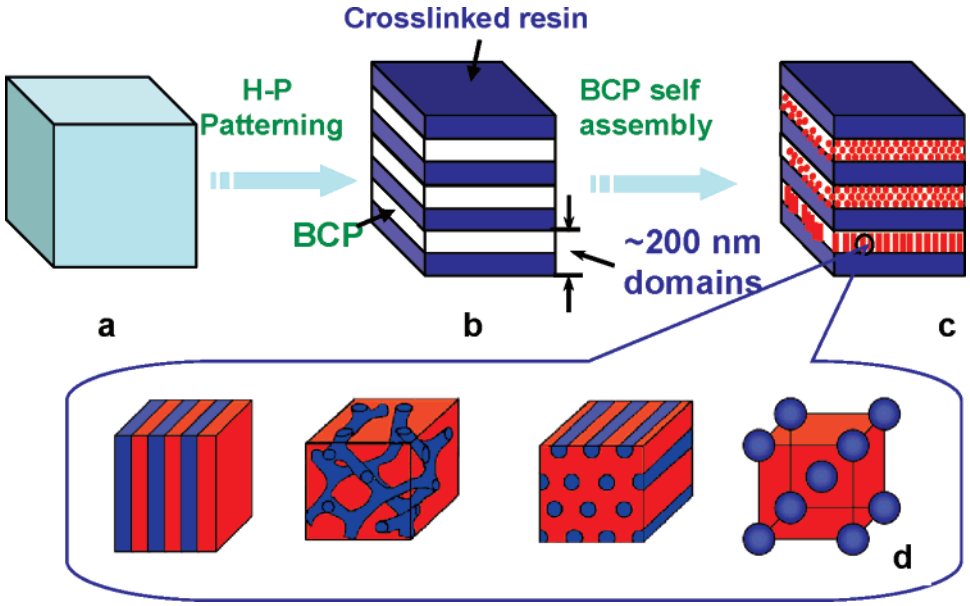

assembly approach can also be combined with soft lithography[12−18] (such as microcontact printing) and electrospinning[19] to achieve smaller feature size in the structure fabricated by current top-down manufacturing techniques. Most of the previous research has focused on maintaining separate processing steps for the two techniques in order to achieve hierarchical structures. Also, discussions of fabrication processes have been limited to 2-D surface structures.

In this Letter, we report the first attempt to combine holographic polymerization (H-P, top-down technique) and BCP self-assembly (bottom-up approach) to create active, tunable hierarchical nanostructures in a volume reflection grating. H-P is a simple, fast, and attractive nanomanufacturing method for fabricating 1-D, 2-D, and 3-D complex photonic structures.[20−24] During the H-P process, a photopolymerizable syrup is exposed to two or more coherent laser beams, interference of which creates a standing wave pattern. Higher intensity regions within the standing wave result in an anisotropic reaction rate and locally faster polymerization process, which in turn leads to a spatial distribution of high-molecular-weight (M_w) polymers. Pure polymer films with a periodic refractive index modulation normal to the film surface (reflection geometry) were first fabricated several decades ago and later formed the commercial basis for DuPont's holographic component product line.[25−27] This unique technique was extended in the mid-1990s by including low-molar-mass, anisotropic liquid crystals (LC) in the monomer syrup. Nonreactive LC, normally ~20−30 (w/w)% of the syrup, continue to be mixed with photopolymerizable monomers, initiators, and surfactants. H-P of this mixture leads to periodically patterned, nanoscale LC droplets, a structure known as holographic polymer-dispersed liquid crystals (H-PDLC).[20] Novel 3-D photonic crystal structures have also been achieved by using multiple-beam configurations.[21−24] Because of the fast kinetics of photopolymerization, these holographic structures can be fabricated within seconds and the symmetry, dimensionality, size, and refractive index modulation can be controlled by the fabrication conditions. In addition to patterning LC, Vaia et al. recently applied this technique to pattern a variety of nanosized objects including gold nanoparticles (5 nm in diameter), polystyrene, latex spheres (260 nm diameter), and silicate nanoplates.[28] We recently demonstrated that the H-P technique can be used to pattern a semicrystalline polymer [poly(ethylene glycol) (PEG)].[29,30] One-dimensional Bragg reflectors were obtained. The reflection spectra of the semicrystalline Bragg reflectors can also be reversibly tuned by varying the temperature.[29,30]

In H-P structures, the feature size is greater than 100 nm. In contrast, BCP are known to self-assemble into a variety of ordered structures (lamella, cylinder, gyroid, body-centered cubic, etc.) on the order of 5−50 nm.[31] Thus, there is enough room in the H-P structure for BCP self-assembly. By combining these two techniques in one system, BCP could be confined in a sub-100 nm nanoenvironment (or scaffold) created by H-P fabrication. Further self-assembly of BCP could lead to hierarchical nano- and microstructures. Scheme 1 shows the schematic representation of this hierarchical fabrication process. In this Letter, as a proof-of-concept, double-crystalline BCP poly(ethylene oxide)-*block*-polycaprolactone (PEO-*b*-PCL, 5*k*/5*k* molecular weight and a polydispersity of 1.06) combined with the thiol-ene photocrosslinkable monomers, were fabricated into hierarchical Bragg reflectors. Profound hierarchical nanostructures were fabricated within a few seconds. The hierarchical structure and morphology were confirmed by using synchrotron small/wide-angle X-ray scattering and transmission electron microscopy techniques. This approach provides a novel platform to fabricate hierarchical nanostructures by combining the top-down and bottom-up techniques.

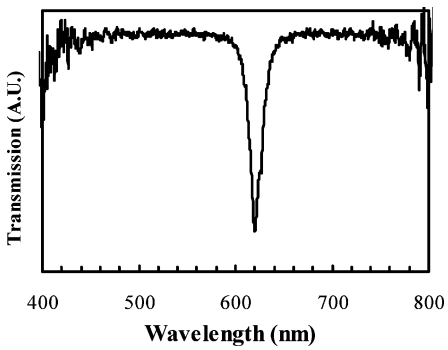

Figure 1. Transmission spectrum of a Norland/PEO-*b*-PCL reflection grating.

Reflection gratings containing PEO-*b*-PCL and crosslinked thiol-ene monomers were fabricated at 80 °C by using a single-beam method to make a 1-D periodic structure from a syrup containing 55 wt % Norland 65, 40 wt % PEO-*b*-PCL, and 5 wt % photoinitiator. Experimental details can be found in the Supporting Information. Figure 1 shows the transmission spectrum of a Norland/PEO-*b*-PCL grating. The sharp notch is evident. The diffraction efficiency of the BCP sample is ~48% according to the depth of the notch. The sharp notch in the transmission spectra suggests that an appreciable refractive index modulation was achieved from the separation of BCP and Norland 65. To confirm this, the morphology of the Bragg reflector was studied by using TEM. Thin sections (~50 nm thick) of the reflection gratings were obtained by microtoming sample films along the film-normal direction. Figure 2a shows a TEM micrograph of a thin section of the Norland/PEO-*b*-PCL grating. RuO_4 was used to stain the sample. The long-range uniform layered structure with alternating dark and light regions can be clearly seen. This morphology is different from that of H-PDLC previously observed based on similar fabrication processes. In the H-PDLC case, phase separation between LC and the polymer resin occurs earlier in the photopolymerization process, leading to the formation of LC droplets ~50−100 nm in the crosslinked resin.[20] In the present case, the BCP formed continuous layers segregated by the Norland resin. This might be due to better compatibility between PEO-*b*-PCL and the Norland resin, which led to slower phase separation kinetics. Therefore, phase separation occurred in the later stages of the polymerization, at which point uniform layered structures were formed. This structure is similar to the uniform layers observed in the Norland/PEG system we previously reported.[29,30] The interface between the resin and the BCP is vague, and it is clear that some of the BCPs are trapped in the resin, confirming the incomplete phase separation. This morphology is consistent with the transmission spectrum results. In Figure 1, nearly 100% background transmission was observed for the Norland/BCP grating, while in a typical H-PDLC grating, significant baseline drop occurs at the low wavelength region (400−500 nm). The baseline drop in the H-PDLC case was attributed to the scattering effect of the nanoscale LC droplets in the H-PDLC structure. In the Norland/PEO-*b*-PCL gratings, BCP and Norland were separated into a continuous layer-by-layer structure, which in turn led to the nearly 100% baseline transmission.[29,30] This uniform layer structure could be of great interest for nanodevice applications.

The alternating layers of Norland and BCP at the submicrometer level leads to the observation of Bragg reflections, as seen in Figure 1. Because the refractive index of Norland is ~1.52 and PEO-*b*-PCL is ~1.46, the grating *d*-spacing can be obtained by:

$$\lambda_0 \approx 2n\Lambda$$

where λ_0 is the position of the notch in Figure 1 and $n \approx (0.6n_{\text{Norland}} + 0.4n_{\text{BCP}})$ is the average refractive index of the thiol-ene polymer and PEO-*b*-PCL. On the basis of the notch positions of the Bragg Reflector shown in Figure 1 and the average refractive index, the resulting grating *d*-spacing, Λ, can be calculated to be ~204 nm, which is consistent with the TEM results.

Upon phase separation between Norland and PEO-*b*-PCL, the PEO-*b*-PCL was confined into ~100 nm thick layers. Within these layers, the BCP has room to microphase separate and form ordered structures on a smaller length scale. The structure of the BCP formed inside the grating is intriguing. Figure 2b shows the enlarged TEM images of Figure 2a. Inside the BCP layer, alternating dark and light lines can clearly be seen. The lines are relatively parallel to the grating layer. There are ~6 dark lines within each BCP layer, and the period is ~17−20 nm. These dark and light lines represent PCL and PEO regions, and the contrast arises from the RuO_4 staining. The alternating lines indicate that PEO and PCL are phase separated within each BCP layer. Because both PEO and PCL are semicrystalline polymers, crystallization occurred as the grating was cooled from the writing temperature (~80 °C) to room temperature (confirmed by DSC experiment, see later discussion). In this particular case, upon crystallization, the PEO and PCL lamellar crystals were formed and aligned parallel to the H-P layers. Therefore, a layer-in-layer hierarchical nanostructure was successfully achieved based on the top-down and bottom-up fabrication techniques. The ordered scales are ~200 and ~20 nm, respectively.

To further confirm the BCP structure and the orientation of the macromolecular chain, SAXS and WAXD experiments were conducted, respectively. The Norland/PEO-*b*-PCL grating cell was opened by using a razor knife, and thin, free-standing films ~15 μm were obtained. Two-dimensional SAXS experiments were carried out with the film oriented parallel and perpendicular to the X-ray beam, and the results are shown in Figure 3a,b. The inset of Figure 3a shows a θ integration of the 2-D pattern. The first- and second-order reflections in the Norland/PEO-*b*-PCL grating corresponds to q ~0.293 and ~0.583 nm^{-1} with a *d*-spacing of ~21 nm for the first-order reflection. This indicates a lamellar structure for the BCP with a period of 21 nm, which is consistent with the TEM observations. The control experiments were performed on the pure PEO-*b*-PCL sample, and a similar lamellar structure was observed. While the X-ray beam was perpendicular to the grating, no small-angle scattering was observed (Figure 3b), indicating that the BCP lamellar normal is perpendicular to the grating layers.

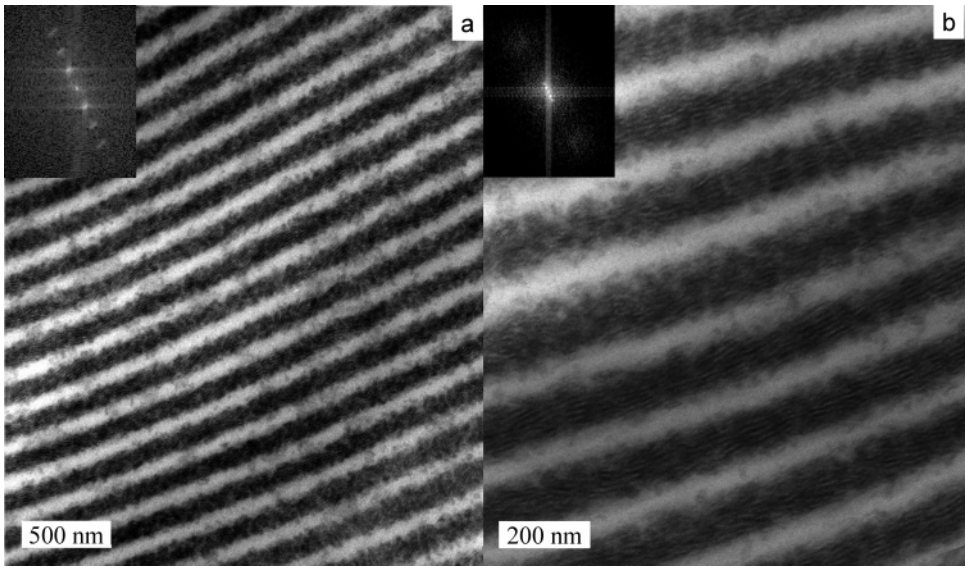

Figure 2. (a) TEM image of the cross section of a Norland/PEO-*b*-PCL grating. (b) Enlarged image of (a), showing the BCP ordering within each grating layer.

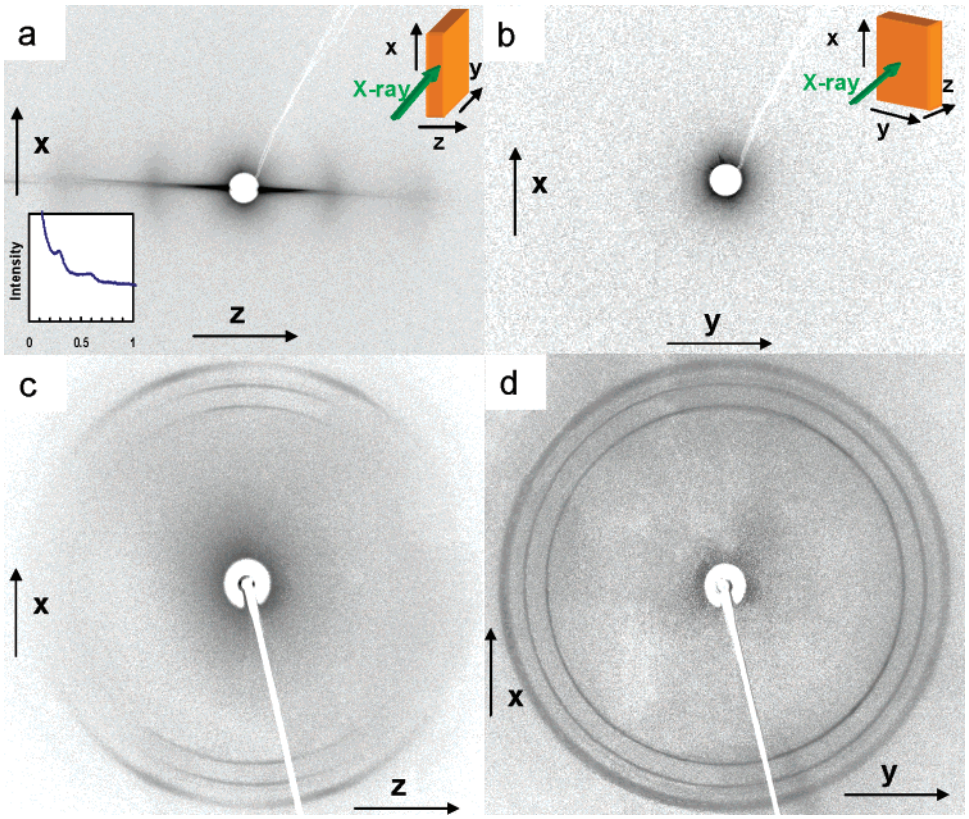

Figure 3. 2-D SAXS (a,b) and 2-D WAXD (c,d) of a Norland/PEO-*b*-PCL reflection grating. The X-ray beam was parallel (a,c) and perpendicular (b,d) to the grating film, as indicated in the top-right insets of (a) and (b).

WAXD and DSC experiments were used to study the crystallization behavior of the free-standing Norland/PEO-*b*-PCL grating. Parts c and d of Figure 3 show the 2-D WAXD patterns with the X-ray beam aligning parallel (Figure 3c) and perpendicular (Figure 3d) to the grating surface, respectively. In Figure 3c, oriented diffraction arcs were observed in the WAXD pattern, while in Figure 3d, only a ring pattern was obtained. Detailed investigation determined that the inner diffraction arcs can be assigned as PEO (120) with a *d*-spacing of 0.494 nm and the outer diffraction can be assigned as the overlap of PEO (−132), (032), (112), (−212), (124), (−204), and (004) reflections with a *d*-spacing of ~0.398 nm.[32] The central diffraction arc located on the meridian with a *d*-spacing of 0.412 nm can be attributed to (110) PCL diffraction.[33,34] Thus, both PEO and PCL are crystallized in the confined nanoenvironments. The DSC experiments also confirmed PEO and PCL crystallization as shown in Figure 4. Both pure PEO-*b*-PCL and

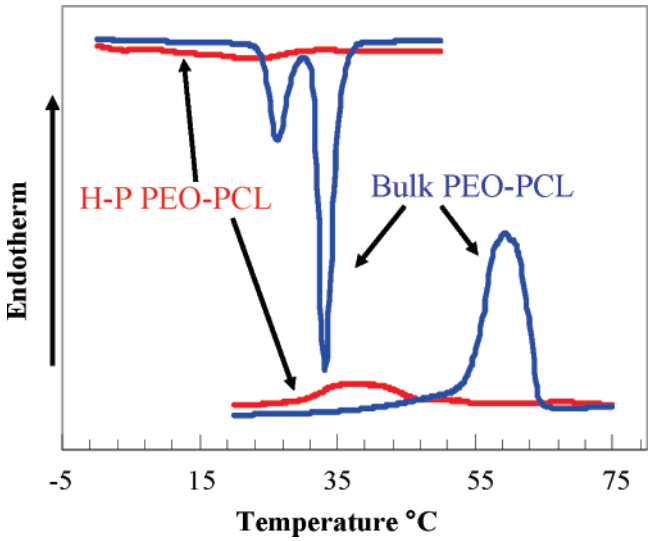

Figure 4. DSC thermograms of pure PEO-*b*-PCL and Norland/PEO-*b*-PCL gratings.

the gratings were subjected to DSC cooling and heating experiments. For pure BCP, two exothermic peaks can be observed at 26 °C and 33 °C during cooling, corresponding to PEO and PCL crystallization, respectively. Upon heating, both PEO and PCL melt at a similar temperature, 59 °C. For the grating sample, much weaker and broader crystallization was observed with a temperature downshift to ~22 °C. The melting peak downshifted to 38 °C. Downshifts of the melting and crystallization temperatures of PEO and PCL can be attributed to the confinement effect of the Norland matrix. This effect is similar to the reported work in the case of semicrystalline BCPs.[29,30] Furthermore, according to our previous studies on the Norland/PEG structure, location of the PEO (120) diffraction on the meridian in the edge-on diffraction pattern suggests that the PEO chains are parallel to the lamellar normal (thus the H-P structure normal).[29,30] The edge-on and flat-on patterns of the PCL (110) peak suggest that the PCL chains are also parallel to the PEO chains and perpendicular to the BCP lamellae/H-P layers. The chain orientation is similar to the confined crystallization of PEO in the poly(ethylene oxide)-*block*-poly(styrene) case.[32,34] The perpendicular chain orientation of the PEG and PCL crystal appears to be in a thermodynamically more stable state at the present crystallization condition. The hierarchical nanostructure of the H-P BCP can be summarized in Figure 5. At the ~200 nm level, lamellar layered structures are formed due to H-P and BCP are confined between the crosslinked resin. Upon cooling, PEO and PCL undergo phase separation/crystallization, resulting in a structure with a period of ~20 nm and both chains are parallel to the layer normal.

It is evident that a layer-in-layer hierarchical structure has been successfully fabricated by combining the top-down H-P and bottom-up BCP self-assembly techniques. There are at least five advantages of this novel nanomanufacturing approach. First, two different nanomanufacturing techniques are seamlessly combined together, and the resulting hierarchical structures span from a few nm to the 200 nm scale.

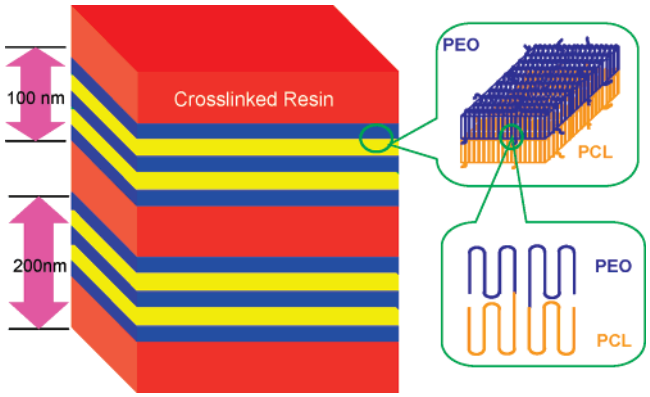

Figure 5. Schematic representation of the hierarchical nanostructures formed by combining H-P and BCP self-assembly.

Second, by combining these two nanomanufacturing techniques, the shortcomings of each method can be overcome: BCP self-assembly helps fabricate a finer structure that H-P cannot achieve, while H-P renders long-range ordering of the BCP self-assembled nanostructures. Third, because of the fast kinetics of H-P, this hierarchical structure can be fabricated in a few seconds. Fourth, compared to other top-down assisted bottom-up approaches, the H-P method enables fabrication of a multiple layered structure, which is critical for 3-D nanodevice applications. Fifth, although the present work only dealt with a 1-D system, a variety of 2-D and 3-D nanostructures can be readily achieved by changing the H-P laser setup. The richness of BCP self-assembled systems also enables innovative structure design with a profound structure hierarchy that can be used for functional devices.

In summary, H-P and BCP self-assembly were combined into one system (Norland/PEO-*b*-PCL) to manufacture layer-in-layer hierarchical nanostructures. Large size, uniform lamellar structures between the crosslinked Norland resin and PEO-*b*-PCL were formed with a period of ~200 nm from the H-P technique. The refractive index modulation between Norland resin and the BCP led to the observation of a reflection notch in the transmission spectra with a diffraction efficiency of ~48%, indicating phase separation of BCP and Norland resin. The nearly 100% background transmission between 400 and 800 nm was attributed to the continuous layer-by-layer structure in the present system. The PEO-*b*-PCL was confined in the Norland resin, and within each BCP region, PEO-*b*-PCL phase separated into a lamellar structure with a period of ~21 nm as determined by the synchrotron SAXS experiment. DSC results suggested that the crystallization of PEO and PCL confined within the Norland matrix showed downshifts of the melting and crystallization temperatures. Synchrotron WAXD showed that PEG and PCL chain axes were parallel to the grating normal. We envisage that a variety of hierarchical nanostructures can be readily fabricated by using our approach.

Acknowledgment. This work was supported by the NRC/US AFOSR Summer Faculty Fellowship, NSF CAREER Award (DMR-0239415) and CMMI-0608953. Synchrotron experiments were conducted at beamline X27C, NSLS in Brookhaven National Laboratory supported by DOE. We

thank Prof. B. S. Hsiao and Dr. Lixia Rong for facilitating the synchrotron X-ray measurement. M.J.B. thanks the NSF GK-12 Fellowship, Drexel University Dean's Fellowship, and Sigma Xi Grants-in-Aid of Research for their support.

Supporting Information Available: Experimental section. This material is available free of charge via the Internet at http://pubs.acs.org.

References

(1) Hawker, C. J.; Russell, T. P. *MRS Bull.* **2005**, *30*, 952.
(2) Li, M.; Coenjarts, C. A.; Ober, C. K. *Adv. Polym. Sci.* **2005**, *190*, 183.
(3) Nalwa, H. S., Ed. *Handbook of Nanostructured Materials and Nanotechnology*; Academic Press: San Diego, CA, 2000; Vol. 1−5.
(4) Roco, M. C., Ed. *Nanotechnology Research Directions: Vision for Nanotechnology R & D in the Next Decade*; National Science and Technology Council ENG-9707092; Kluwer Academic Publishers: Dordrecht, The Netherlands, 2000.
(5) Muthukumar, M.; Ober, C. K.; Thomas, E. L. *Science* **1997**, *277*, 1225.
(6) Park, C.; Yoon, J.; Thomas, E. L. *Polymer* **2003**, *44*, 6725−6760.
(7) Tenneti, K. K.; Chen, X. F.; Li, C. Y.; Wan, X.; Fan, X.; Zhou, Q. F.; Rong, L.; Hsiao, B. *Macromolecules* **2007**, *40*, 5095.
(8) Tenneti, K. K.; Chen, X. F.; Li, C. Y.; Wan, X.; Zhou, Q. F.; Sics, I.; Hsiao, B. *J. Am. Chem. Soc.* **2005**, *127*, 15481−15490.
(9) Kim, S. O.; Solak, H. H.; Stoykovich, M. P.; Ferrier, N. J.; De Pablo, J. J.; Nealey, P. F. *Nature* **2003**, *424*, 411.
(10) Cheng, J. Y.; Ross, C. A.; Smith, H. I.; Thomas, E. L. *Adv. Mater.* **2006**, *18*, 2505.
(11) Blaaderen, A. v.; Ruel, R.; Wiltzius, P. *Nature* **1997**, *385*, 321.
(12) Pai, R. A.; Humayun, R.; Schulberg, M. T.; Sengupta, A.; Sun, J.-N.; Watkins, J. J. *Science* **2004**, *303*, 507.
(13) Bal, M.; Ursache, A.; Tuominen, M. T.; Goldbach, J. T.; Russell, T. P. *Appl. Phys. Lett.* **2002**, *81*, 3479.
(14) Spatz, J. P.; Chan, V. Z.-H.; Mossmer, S.; Kamm, F.-M.; Plettl, A.; Ziemann, P.; Moller, M. *Adv. Mater.* **2002**, *14*, 1827.
(15) Glass, R.; Arnold, M.; Blummel, J.; Kuller, A.; Moller, M.; Spatz, J. P. *Adv. Funct. Mater.* **2003**, *13*, 7, 569.
(16) Yao, J.; Yan, X.; Lu, G.; Zhang, K.; Chen, X.; Jiang, L.; Yang, B. *Adv. Mater.* **2004**, *16*, 81.
(17) Yun, S.-H.; Sohn, B.-H.; Jung, J. C.; Zin, W.-C.; Ree, M.; Park, J. W. *Nanotechnology* **2006**, *17*, 450.
(18) Moon, J. H.; Kim, W. S.; Ha, J.-W.; Jang, S. G.; Yang, S.-M.; Park, J.-K. *Chem. Commun.* **2005**, 4107.
(19) Ma, M.; Hill, R. M.; Lowery, J. L.; Fridrikh, S. V.; Rutledge, G. C. *Langmuir* **2005**, *21*, 5549.
(20) Bunning, T. J.; Natarajan, L. V.; Tondiglia, V. P.; Sutherland, R. L. *Annu. Rev. Mater. Sci.* **2000**, *30*, 83.
(21) Tondiglia, V. P.; Natarajan, L. V.; Sutherland, R. L.; Tomlin, D.; Bunning, T. J., *Adv. Mater.* **2002**, *14*, 187−191.
(22) Campbell, M.; Sharp, D. N.; Harrison, M. T.; Denning, R. G.; Turberfield, A. J. *Nature* **2000**, *404*, 53.
(23) Sutherland, R. L.; Tondiglia, V. P.; Natarajan, L. V.; Chandra, S.; Tomlin, D.; Bunning, T. J. *Opt. Express* **2002**, *10*, 1074.
(24) Escuti, M. J.; Qi, J.; Crawford, G. P. *Opt. Lett.* **2003**, *28*, 522.
(25) Colburn, W. S.; Haines, K. A. *Appl. Opt.* **1971**, *10*, 1636.
(26) Gambogi, W. J.; Weber, A. M.; Trout, T. J. *SPIE Proc.* **1994**, *2043*, 2.
(27) Smothers, W. K.; Moroe, B. M.; Weber, A. M.; Keys, D. E. *SPIE Proc.* **1990**, *1212*, 20.
(28) Vaia, R. A.; Dennis, C. L.; Natarajan, L. V.; Tondiglia, V. P.; Tomlin, D. W.; Bunning, T. J. *Adv. Mater.* **2001**, *13*, 1570.
(29) Li, C. Y.; Birnkrant, M. J.; Natarajan, L. V.; Tondiglia, V. P.; Lloyd, P. F.; Sutherland, R. L.; Bunning, T. J. *Soft Matter* **2005**, *1*, 238.
(30) Birnkrant, M. J.; McWilliams, H. K.; Li, C. Y.; Natarajan, L. V.; Tondiglia, V. P.; Lloyd, P. F.; Sutherland, R. L.; Bunning, T. J. *Polymer* **2006**, *47*, 8147.
(31) Bates, F. S.; Fredrickson, G. H. *Annu. Rev. Phy. Chem.* **1990**, *41*, 525.
(32) Zhu, L.; Calhoun, B. H.; Ge, Q.; Quirk, R. P.; Cheng, S. Z. D.; Thomas, E. L.; Hsia, B. S.; Yeh, F.; Liu, L.; Lotz, B. *Macromolecules* **2001**, *34*, 1244.
(33) Bittiger, H.; Marchessault, R. H.; Niegisch, W. D. *Acta Crystallogr., Sect. B: Struct. Sci.* **1970**, *26*, 1923.
(34) Shin, D.; Shin, K.; Aamer, K. A.; Tew, G. N.; Russel, T. P. *Macromolecules* **2005**, *38*, 104.

NL071673J